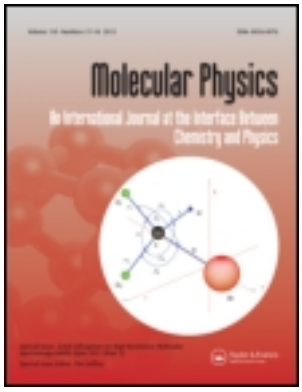

Molecular Physics: An International Journal at the Interface Between Chemistry and Physics
Publication details, including instructions for authors and subscription information:
http://www.tandfonline.com/loi/tmph20

Quantum capture of charged particles by rapidly rotating symmetric top molecules with small dipole moments: analytical comparison of the fly-wheel and adiabatic channel limits

M. Auzinsh [a], E. I. Dashevskaya [b c], E. E. Nikitin [b c] & J. Troe [c d]
[a] Department of Physics, University of Latvia, Riga, Latvia
[b] Schulich Faculty of Chemistry, Technion - Israel Institute of Technology, Haifa, Israel
[c] Max-Planck-Institut für Biophysikalische Chemie, Göttingen, Germany
[d] Institut für Physikalische Chemie, Universität Göttingen, Göttingen, Germany
Accepted author version posted online: 13 Mar 2013.Published online: 02 Sep 2013.

To cite this article: M. Auzinsh, E. I. Dashevskaya, E. E. Nikitin & J. Troe (2013) Quantum capture of charged particles by rapidly rotating symmetric top molecules with small dipole moments: analytical comparison of the fly-wheel and adiabatic channel limits, Molecular Physics: An International Journal at the Interface Between Chemistry and Physics, 111:14-15, 2003-2011, DOI: 10.1080/00268976.2013.780101

To link to this article: http://dx.doi.org/10.1080/00268976.2013.780101

Molecular Physics, 2013
Vol. 111, Nos. 14–15, 2003–2011, http://dx.doi.org/10.1080/00268976.2013.780101

INVITED ARTICLE

Quantum capture of charged particles by rapidly rotating symmetric top molecules with small dipole moments: analytical comparison of the fly-wheel and adiabatic channel limits

M. Auzinsh[a], E.I. Dashevskaya[b,c], E.E. Nikitin[b,c] and J. Troe[c,d,*]

[a]*Department of Physics, University of Latvia, Riga, Latvia;* [b]*Schulich Faculty of Chemistry, Technion – Israel Institute of Technology, Haifa, Israel;* [c]*Max-Planck-Institut für Biophysikalische Chemie, Göttingen, Germany;* [d]*Institut für Physikalische Chemie, Universität Göttingen, Göttingen, Germany*

(*Received 2 January 2013; final version received 20 February 2013*)

The rate coefficients for capture of charged particles by spherical top molecules, which by isotopic substitution become symmetric top molecules with small dipole moment, are expressed analytically for the two limiting cases of weak coupling of the molecular angular momentum to the collision axis (dominating Coriolis interaction, the fly-wheel [FW] approximation) and strong coupling (negligible Coriolis interaction, the adiabatic channel [AC] approximation). The comparison leads to relations between rate coefficients for ultra-low (FW) and moderate (AC) temperatures and defines the range of parameters for which the analytical expressions become insufficient and a numerical treatment is necessary.

Keywords: collision dynamics; adiabatic channels; capture processes

1. Introduction

The problem of the capture of charged particles by dipolar molecules is of interest in the field of ion–molecule reactions and electron attachment processes involving complex formation (see, e.g., [1,2]). If the molecules are rapidly rotating, i.e., if the Massey parameters (the products of characteristic frequencies with respect to transitions between different rotational molecular states and the characteristic collision time) are large, the capture problem can be treated within the adiabatic channel (AC) model [3]. This approach was used in the perturbed rotational (PR) state method [4], the adiabatic invariance (AI) method [5] and the adiabatic capture centrifugal sudden (ACCS) approximation [6]. As all of these models were shown to be equivalent to each other, numerical differences were due to more or less adequate calculational simplifications [7,8]. The applicability of the AC approach and the definition of the respective Massey parameters were discussed in Nikitin and Troe [9] in connection to different temperature regimes – ultra-low, low and moderate. However, even if the Massey parameters for transitions between different rotational states are large, there exists yet another prerequisite for the application of the AC approximation: the AC potentials at the inter-particle distances R important for capture need to be defined unambiguously by locking of the molecular angular momentum j to the collision axis. This locking implies the transformation from an asymptotic set of quantum numbers J, j, ℓ to a set of quantum numbers J, j, m for the 'collision complex' [10]. The locking distance $R_{\rm L}$ is roughly determined by the condition that the frequency of rotation $\omega_{\rm rot}(R, J)$ of the collision axis at total angular momentum J is about equal to the characteristic precession frequency $\omega_{\rm prec}(R, \boldsymbol{j})$ of $\boldsymbol{j}$ about R. The uncertainty δR_L in the locking distance $R_{\rm L}$, the latter being found from the condition

$$\omega_{\rm rot}(R_{\rm L}, J) = \omega_{\rm prec}(R_{\rm L}, j), \tag{1}$$

is small (i.e. $\delta R_L \ll R_L$) when the anisotropic potential, with increasing R, decreases faster than the centrifugal energy that falls as R^{-2}. For relatively slowly decreasing potentials, e.g., for charge–quadrupole or resonance dipole–dipole interactions (falling as R^{-3}), the ratio $\delta R_L/R_L$ is not small enough to assure a sudden locking of j to R in the locking region. This leads to some specific features of the complex formation such as discussed in Dashevskaya et al. [11] and Nikitin and Troe [12].

If the inter-particle interaction, on the other hand, is of first-order charge–dipole type, as is the case for a symmetric top molecule for $j > 0$ (for $j = 0$, the first-order charge–dipole interaction disappears), $\omega_{\rm prec}(R, j)$ decreases as R^{-2} and Equation (1) has no solution for finite R_L. Although this indicates a difficulty in employing AC potentials, the latter have been defined and used in classical calculations of capture cross-sections and rate coefficients under the condition $J \gg j$ [13–15]. Then, the difference between J and ℓ disappears, and with it appears the possibility to label asymptotic states by J and m (i.e. the projection of $\boldsymbol{j}$ onto the collision axis $\boldsymbol{R}$). In the adiabatic approximation with

*Corresponding author. Email: shoff@gwdg.de

respect to the states of the rotor with quantum numbers j, k (with k being the quantum number of the projection of $\boldsymbol{j}$ onto the symmetry axis of the top), the charge–dipole interaction is determined by the projection of the average dipole moment $\bar{\mu}_D(j,k) = \mu_D k/\sqrt{j(j+1)}$ (which is directed along $\boldsymbol{j}$) onto the collision axis. Then, the capture condition, for pure charge–dipole interaction, is written as $J \leq J_c$, where J_c is determined from the balance of the centrifugal repulsion and the electrostatic attraction of the partners. Qualitatively, this condition approximately reads

$$\frac{\hbar^2 J_c^2}{2\mu R^2} \approx \frac{q\bar{\mu}_D}{R^2}, \tag{2}$$

where μ is the reduced mass of the collision pair and q is the charge of the ion. The value of J_c then is of the order $J_c \approx \sqrt{2\delta}$, where δ is a dimensionless characteristic parameter,

$$\delta = q\mu\bar{\mu}_D/\hbar^2. \tag{3}$$

If $\bar{\mu}_D \approx 1$ a.u. (for a typical polar molecule) and $\mu \approx 10^4$ a.u. (collisions with an ion of 10 atomic mass), the value of J_c is about 10^2, which validates the use of the classical approximation. However, for molecules with very small dipole moments that arise, for instance, from isotopic substitution of one of the atoms of the spherical top (see Appendix), J_c can be of the order unity. Then, a quantum treatment of capture becomes necessary that takes into account a partial locking of j to R, and even goes (for very small $\bar{\mu}_D$) to the limit where j is almost decoupled from R (the so-called free-wheel [FW] limit of charge–quadrupole [11] and resonance dipole–dipole [12,16] interactions).

The aim of the present work is to study rate coefficients for capture of charged particles by symmetric top molecules with small dipole moments at low collision energies and temperatures by using two limiting analytical approaches, the FW approximation in the quantum collision regime (ultra-low temperatures) and the AC approximation for the adjacent classical regime (moderate temperatures), considering the case of an anisotropic first-order charge–dipole interaction on the background of an isotropic charge-induced dipole interaction. Of particular interest is the question at which energies (or temperatures) the transition from the FW to the AC regime is located.

The plan of the paper is the following. Section 2 describes calculations with the FW interaction. In Sections 3 and 4, we discuss the quantum s-wave FW and classical AC rate coefficients. Section 5 compares the quantum and classical calculations and defines the region where results bridging the FW and AC limits are needed. Section 6 concludes the paper. Appendix presents a simple model for estimation of the small dipole moments for symmetric top molecules that originate from spherical tops upon isotopic substitution of one of its atoms.

2. Fly-wheel potential

The FW approximation to the capture with an anisotropic interaction potential is obtained by developing a perturbation theory with respect to the charge–dipole interaction in the basis of free wave functions, for both intrinsic and relative rotation. The perturbation approach is valid for molecules with small dipole moments. The physical reason for the existence of small dipole moments (and their possible range) for symmetric top molecules is discussed in Appendix. In general, the FW potential remains isotropic in the succession of perturbation orders, but each step defines a new basis, the states of which are coupled by radial motion of the partners. The simplification of using the FW approach is attained either when one can restrict oneself to the lowest order or when the improved basis functions are weakly coupled by the radial motion of the partners. The former applies to charge–quadrupole [11] and resonance dipole–dipole [12,16] interactions, when higher-order corrections can be neglected because they fall off faster with increasing R than the leading second-order term. The latter applies to charge–dipole interactions, when the dominant change in the basis is R-independent and the leading terms of higher-order corrections fall off similarly as the leading second-order term, being proportional to R^{-2}. Each order of the series representation of the interaction starts with a R^{-2} term, which is followed by correction terms proportional to R^{-4}, R^{-6} etc. The former arises from the virtual transitions $j, k, \ell \to j', k', \ell'$, with $j, k = j', k'$, and the latter from $j, k \neq j', k'$. In the following, the correction terms that fall faster than R^{-4} are neglected, while those proportional to R^{-4} can be accounted for by simple renormalisation of the polarisability α of the top, making it j, k-dependent [13,15]. Since in the scaled variables, α disappears (see below), we will not dwell on this point, and concentrate only on the leading term of the effective interaction that arises from the virtual transitions $j, k, \ell \to j, k, \ell'$ and which features the R^{-2} dependence. Here, the application of the central-field higher-order FW potential is limited only by the convergence of the perturbation series with respect to the parameter responsible for the charge–dipole interaction.

Within the above approximations, the effective anisotropic interaction, taken to be diagonal in the quantum numbers j, k is written as

$$\hat{V} = \frac{\hbar^2 \hat{\mathbf{l}}^2}{2\mu R^2} + q\bar{\mu}_D(j,k)\frac{\hat{\mathbf{j}}}{\sqrt{j(j+1)}}\frac{\mathbf{R}}{R^3} - \frac{q^2\alpha}{2R^4}. \tag{4}$$

The first term on the right-hand side (r.h.s.) of Equation (4) is the centrifugal energy expressed through the operator of the relative angular momentum, the second is the weak-field charge–dipole interaction containing the projection of the average dipole moment directed along the vector $\boldsymbol{j}$ onto the collision axis $\boldsymbol{R}$, and the third is the charge-induced dipole interaction. If $\boldsymbol{R}$ is taken as the quantisation axis

in the J, j, m representation, and $\bar{\mu}_D(j,k)$ is expressed as $\bar{\mu}_D(j,k) = \mu_D k/\sqrt{j(j+1)}$ (see Section 1), the first and the second terms on the r.h.s. of Equation (4) yield the familiar expressions for their expectation values used in the AC treatment [13,15]:

$$\left\langle J, j, m \left| \frac{\hbar^2 \hat{\mathbf{l}}^2}{2\mu R^2} \right| J, j.m \right\rangle = \frac{\hbar^2}{2\mu R^2}(J(J+1) - 2m^2 + j(j+1))$$

$$\left\langle J, j, m \left| \frac{q\bar{\mu}_D}{\sqrt{j(j+1)}} \frac{\hat{\mathbf{j}}\mathbf{R}}{R^3} \right| J, j, m \right\rangle = \frac{q\mu_D km}{j(j+1)R^2} \qquad (5)$$

However, in our case, the axis R is not a good quantisation axis, and therefore, we prefer to deal with the interaction in its operator form, as in Equation (4), rather than in the form of expectation values as normally used in the AC treatment. Then, passing to the scaled quantities $\rho = R/R_L$ and $\varepsilon = E/E_L$ for the distance and the energy as well as $\kappa = kR_L$ for the wave vector (with $R_L = q\sqrt{\mu\alpha}/\hbar$ and $E_L = \hbar^2/\mu R_L^2$), the scaled interaction $\hat{\upsilon} = \hat{V}/E_L$ assumes the form

$$\hat{\upsilon}(\rho) = \frac{\hat{\mathbf{l}}^2}{2\rho^2} + \frac{\delta\hat{\mathbf{j}}\boldsymbol{\rho}}{\sqrt{j(j+1)}\rho^3} - 1/2\rho^4. \qquad (6)$$

The FW potential for fixed quantum numbers J, j, k is now written as a perturbation series with respect to the charge–dipole interaction in the J, j, k, ℓ basis for a space-fixed quantisation axis. With the quantum number ℓ specifying the zero-order term of the perturbation series, the effective potential between an ion and a rotor in the rotational state j, k (with k implicitly included in δ from Equation (3)) for the total angular momentum J, ${}^{\mathrm{FW}}\upsilon_\ell^{(J,j)}(\rho)$, becomes

$${}^{\mathrm{FW}}\upsilon_\ell^{(J,j)}(\rho) = {}^{\mathrm{FW}}c_\ell^{(J,j)}(\delta)/2\rho^2 - 1/2\rho^4. \qquad (7)$$

The coefficients ${}^{\mathrm{FW}}c_\ell^{(J,j)}(\delta)$ start with the zero-order term $\ell(\ell+1)$ arising from the first term on the r.h.s. of Equation (6), while other terms are calculated as a perturbation series with respect to the interaction represented by the second term in the r.h.s. of Equation (6). Here, ℓ runs from $|J-j|$ to $J+j$ and, in the case $J=j$, it starts from $\ell = 0$. We now concentrate on the latter case, which is appropriate for perturbed s-wave scattering where the effective potential is attractive since the zero-order term disappears. For higher waves, with $\ell > 0$, the effective potential, for small δ, is repulsive at large distances, such that the capture at low collision energies does not take place.

We have calculated ${}^{\mathrm{FW}}c_0^{(j,j)}(\delta)$ analytically up to fourth order using the standard techniques [17]. The result read

$${}^{\mathrm{FW}}c_0^{(j,j)}(\delta) = -\frac{2}{3}\delta^2 + \frac{2}{9}\left(\frac{11}{15} + \frac{1}{5j(j+1)}\right)\delta^4 + O(\delta^6). \qquad (8)$$

It is noteworthy that the series representation of ${}^{\mathrm{FW}}c_0^{(j,j)}(\delta)$ in Equation (8) performs well at $\delta = \delta^* = 0.64$ when ${}^{\mathrm{FW}}c_0^{(j,j)}(\delta)$ nearly equals $-1/4$ and the capture channel for the attractive R^{-2} interaction opens up ([18], section 35). This can be judged from the consecutive values of the terms for $\delta = \delta^*$ on the r.h.s. of Equation (8). We thus expect that the FW approximation in the form of Equation (8) is applicable for the description of capture at values of δ below ($\delta < \delta^*$) and slightly above ($\delta > \delta^*$) the threshold. In the latter case, the representation of ${}^{\mathrm{FW}}c_0^{(j,j)}(\delta)$ by Equation (8) might be worse, but this does not affect the capture probability since the latter quickly levels off to its maximal value of unity (the so-called unitary limit). With this feature of the probability, the expression in Equation (8) can be safely used up to $\delta = 1$ (see below). For higher values of δ, the series expression for ${}^{\mathrm{FW}}c_0^{(j,j)}(\delta)$ in Equation (8) diverges as indicated by the change in the qualitative behaviour of ${}^{\mathrm{FW}}c_0^{(j,j)}(\delta)$ (from decreasing to increasing). Besides, for $\delta > 1$, the FW capture rate coefficient, beyond the leading s-wave term, will be contaminated by higher waves, which are neglected in this work. Since the convergence of the perturbation series is an important point of the present treatment, we have numerically calculated, within the basis $J = j$, the lowest eigenvalue $c_0^{(j,j)}(\delta)$ of the operator $\hat{\mathbf{l}}^2 + 2\delta\hat{\mathbf{j}}\boldsymbol{\rho}/\sqrt{j(j+1)}\rho$ that, if represented as a series in δ, generates ${}^{\mathrm{FW}}c_0^{(j,j)}(\delta)$. The results are shown in Figure 1 by the curves for $j = 1$ and $j \geq 3$ (with that for $j = 2$ lying between them), where the quadratic and quartic approximations from Equation (8) are compared with accurate numerical results. We see that the above prediction of a good performance of the perturbation series for $\delta < 1$ is substantiated by the accurate numerical results.

We conclude from Equation (8) and from Figure 1 that ${}^{\mathrm{FW}}c_0^{(j,j)}(\delta)$ depends on j rather weakly. This has the following practical significance. Extrapolating the results to higher j (and, therefore, to higher $J = j$), we observe that the quantity J then can be considered as a classical vector, and its direction can be taken as the quantisation axis for the relative angular momentum vector $\hat{\mathbf{l}}$. In other words, the quantity ${}^{\mathrm{FW}}c_0^{(j,j)}(\delta)|_{j>>1} = {}^{\mathrm{FW}}c_0(\delta)$ can be regarded as the lowest eigenvalue of the operator $\hat{\mathbf{l}}^2 + 2\delta\cos\gamma$, where γ is the angle between $\boldsymbol{\rho}$ and the quantisation axis. The δ dependence of the lowest eigenvalue of this operator was studied in Dashevskaya et al. [19], where it was represented as $D_s(d)$ (with $d = \delta$). This observation makes it possible to use the results of the numerical fitting of the electron–molecule capture probabilities in Dashevskaya

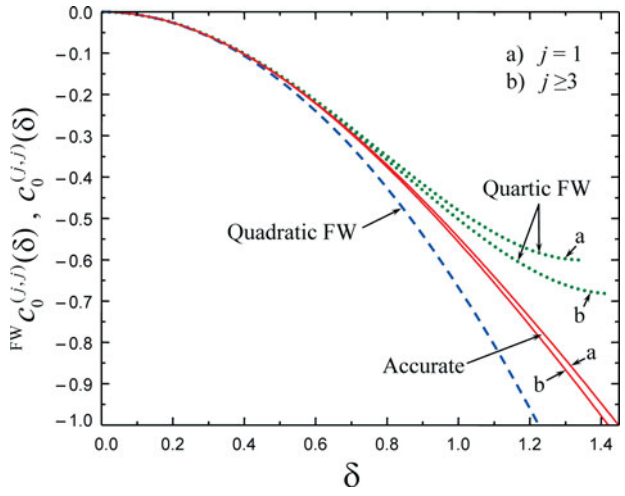

Figure 1. Comparison of the series representation of $^{FW}c_0^{(j,j)}(\delta)$ from Equation (8) with accurate results for the lowest eigenvalue $c_0^{(j,j)}(\delta)$ of the operator $\hat{\mathbf{l}}^2 + 2\delta\hat{\mathbf{j}}\boldsymbol{\rho}/\sqrt{j(j+1)}\rho$ in the $J = j$ basis. Notes: Shown are the accurate results for $j = 1$ (red curve a) and $j \geq 3$ (red curve b), with the results for $j = 2$ lying between them (not shown). The dashed blue line corresponds to the j-independent quadratic approximation, and the green dotted lines correspond to the j-dependent quartic approximation from Equation (8).

et al. [20] within the sudden approximation for approximate calculations of the ion–molecule capture probabilities within the adiabatic approximation; see the following section.

3. *s*-wave FW capture probabilities, cross-sections and rate coefficients

The s-wave capture in the field of the $^{FW}\upsilon$ potential is calculated from the Schroedinger equation, which, in terms of the scaled variables $\rho = R/R_L$ and $\kappa = kR_L$, takes the form

$$\left\{-\frac{d^2}{2d\rho^2} + \frac{^{FW}c_0(\delta)}{2\rho^2} - \frac{1}{2\rho^4}\right\}\psi(\rho,\kappa) = \frac{\kappa^2}{2}\psi(\rho,\kappa). \tag{9}$$

Two points deserve mention:

(1) The lack of a dependence of $^{FW}c_0(\delta)$ on j in Equation (9) means that the capture probability $^{FW}P(\kappa,\delta)$ derived from Equation (9) does not depend on j.
(2) The equality $^{FW}c_0(\delta) = D_s(d)|_{d=\delta}$ means that analytical expressions for capture probabilities, for different values of D_s depending on d, apply as well to $^{FW}P(\kappa,\delta)$.

Explicitly, (i) and (ii) imply that the capture probabilities $^{FW}P(\kappa,\delta)$ can be identified with the fitting analytical expressions for $P_{0,0}^{app}(\kappa,d)$ from equations (3)–(8) of Dashevskaya et al. [20] or obtained by a direct numerical integration of the capture equation (Equation (9)) with j-independent coefficient $^{FW}c_0(\delta) = -2\delta^2/3 + 22\delta^4/135$.

The probabilities, $^{FW}P(\kappa,\delta)$, in turn, define the scaled s-wave j-independent rate coefficient $^{FW}\chi_s(\kappa,\delta)$, i.e., the ratio of the κ-dependent dependent rate coefficient to the κ-independent Langevin rate coefficient $k_L = 2\pi q(\alpha/\mu)^{1/2}$, as

$$^{FW}\chi_s(\kappa,\delta) = \left(1/2\kappa\right)^{FW}P(\kappa,\delta). \tag{10}$$

In the absence of charge–dipole interaction (i.e. for $\delta = 0$), Equation (10) can be approximated analytically by the expression

$$^{FW}\chi_s(\kappa,\delta)\big|_{\delta=0} = \frac{1 - 0.25\exp(-1.387\kappa) - 0.75\exp(-4.871\kappa)}{2\kappa}, \tag{11}$$

(see equation (2.5) of Dashevskaya et al. [19]) which gives the correct Vogt–Wannier limit of $^{FW}\chi_s(\kappa,\delta)\big|_{\substack{\delta=0,\\ \kappa=0}} = 2$ for $\kappa \to 0$ (corresponding to the Bethe limit of a finite value of the rate coefficient at $\kappa \to 0$) and the maximal s-wave rate coefficient for $\kappa \gg 1$. For strong charge–dipole interaction (large δ), Equation (10) approaches the unitary limit for arbitrary κ, i.e.

$$^{max}\chi_s(\kappa) = {}^{FW}\chi_s(\kappa,d)\big|_{\delta\gg\delta^*} = 1/2\kappa, \tag{12}$$

and shows a $1/\kappa$ divergence as $\kappa \to 0$. This divergence represents a violation of the Bethe condition of a finite value of the rate coefficient at $\kappa \to 0$.

The requirement of large δ for Equation (12) to be valid should be compatible with the requirement that the FW representation of the interaction potential is still valid. As a compromise between these two conditions, we consider the range $0 < \delta < 1$. For the maximal value of δ in this range, i.e.$\delta_{max} = 1$, the probability $^{FW}P(\kappa,\delta)\big|_{\delta=1}$ is close to unity (see figure 4 from Dashevskaya et al. [20]).

The s-wave FW rate coefficients, $^{FW}\bar{\chi}_s(\theta,\delta)$, are obtained by averaging of $^{FW}\chi_s(\kappa,\delta)$ through

$$^{FW}\bar{\chi}_s(\theta,\delta) = \int_0^\infty {}^{FW}\chi_s(\kappa,\delta)F(\kappa,\theta)d\kappa \tag{13}$$

over the Boltzmann distribution

$$F(\kappa,\theta) = (2\pi\theta)^{-1/2}\exp(-\kappa^2/2\theta)\frac{2\kappa^2}{\theta} \tag{14}$$

that contains the scaled temperature

$$\theta = \left(q^2\mu^2\alpha/\hbar^4\right)k_BT. \tag{15}$$

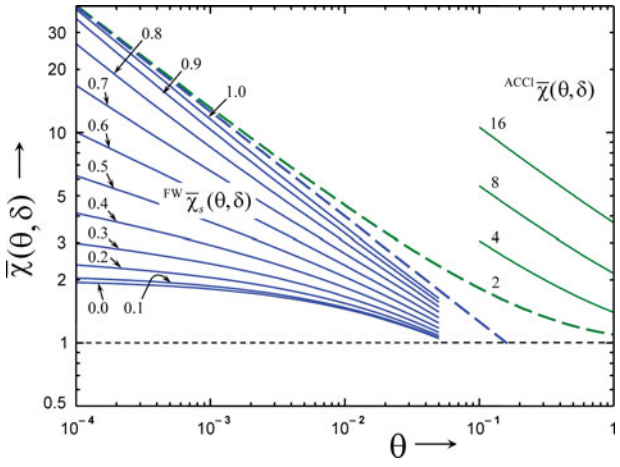

Figure 2. Comparison of s-wave FW (left-hand area, full blue lines) and classical AC capture rate coefficients (right-hand area, full green lines)
Notes: The curves are labelled by the values of δ; see text. The dashed lines stand for $^{FW}\bar{\chi}_s^{max}(\theta)$ and $^{ACCI}\bar{\chi}^{min}(\theta)$ rate coefficients. The intermediate area corresponds to the range of parameters θ and δ not covered by the present analytical treatment. The horizontal dashed black line corresponds to the Langevin rate coefficient.

With analytical formulae for the probabilities, the calculation of $^{FW}\bar{\chi}_s(\theta,\delta)$ can be easily performed by direct integration. In particular, the maximal FW rate coefficient that corresponds to the unitary limit is

$$^{FW}\bar{\chi}_s^{max}(\theta) = 1/\sqrt{2\pi\theta}. \tag{16}$$

Graphs of $^{FW}\bar{\chi}_s(\theta,\delta)$ versus θ for $0 < \delta < 1$ are shown in Figure 2 by full blue lines up to $\theta = 0.05$, where $^{FW}\bar{\chi}_s(\theta,\delta)$ are still visibly larger than the Langevin asymptotics (dashed black line). The graph of $^{FW}\bar{\chi}_s^{max}(\theta)$, extended until its crossing with the Langevin asymptotics, corresponds to the dashed blue line. With the thermally averaged counterparts of $^{FW}\chi_s(\kappa)$ from Equation (11) and of $^{FW}\bar{\chi}_s^{max}(\theta)$ from Equation (16), the δ dependence of $^{FW}\bar{\chi}_s(\theta,\delta)$ can be approximately represented by the interpolation formulae from Dashevskaya et al. [19]. In particular, at very low temperatures, the $^{FW}\bar{\chi}_s(\theta,\delta)$ are proportional to $\theta^{-\gamma}$, where $\gamma = \sqrt{^{FW}c_0 + 1/4} - 1/2$ and $-1/4 < {}^{FW}c_0 \le 0$. Note that γ is smaller than 0.5, which implies a slower divergence of $^{FW}\bar{\chi}_s(\theta,\delta)$ than that of $^{max}\bar{\chi}_s(\theta)$, which in turn is the same as that of the classical AC rate coefficient (see Section 5). As an interesting observation, we mention that at $^{FW}C_0 = -1/4$ (which corresponds to $\delta = \delta^* = 0.64$) when the channel for the pure charge–dipole interaction becomes completely open, the capture rate coefficient $^{FW}\bar{\chi}_s(\theta,\delta^*)$ is still noticeably lower that $^{max}\bar{\chi}_s(\theta)$. We interpret this as a consequence of the partial reflection of the incoming s-wave travelling across the long-range charge–dipole attractive potential proportional to ρ^{-2} from the short-range drop caused by the charge-induced dipole potential proportional to ρ^{-4}.

Finally, we note that the divergence of $^{FW}\bar{\chi}_s(\theta,\delta)$ at $\theta \to 0$ is the result of the adopted approximation that the states with the quantum numbers k and $-k$ (or the states with given $|k|$ and different parity) are degenerate. This degeneracy may be lifted by certain interactions (e.g. hyperfine coupling) that lead to the K-doubling phenomenon. The K-doubling can be neglected if the non-adiabatic coupling between the two components falls into the sudden regime, and it certainly cannot be neglected if the collision energy is comparable to the K-doubling splitting. For the CH_3D molecule, considered in Section 5, the K-doubling splitting is in the kilohertz (kHz) range [21], implying that the K-doubling feature, for $CH_3D + H^+$ capture, has to be taken into account only at extremely low temperatures. A rough estimate of the limiting zero-temperature capture rate coefficient, ignoring all fine details of hyperfine coupling, can be obtained by the perturbation approach, by calculating the increase in the effective polarisability, which is due to the mixing of the K-doublet components by the electric field of the impinging ion. Standard calculations show that the FW interaction $\propto R^{-2}$ transforms into a K-doublet charge-induced dipole interaction $\propto R^{-4}$. When this term is combined with the conventional charge-induced dipole interaction, it implies an increase in the polarisability α by a quantity $\Delta\alpha$, which is of the order of $\delta^2/\Delta\varepsilon$, where $\Delta\varepsilon$ is the K-doubling spacing (in scaled units). Therefore, in the limit $\kappa \to 0$, where the condition $\kappa^2/2 \ll \Delta\varepsilon$ is automatically satisfied, the VW rate coefficient $^{VW}\chi$ should be replaced by an 'effective VW' (EVW) rate coefficient $^{EVW}\chi$

$$^{VW}\chi = 2 \to {}^{EVW}\chi = 2\sqrt{1 + \Gamma\delta^2/\Delta\varepsilon\alpha}, \tag{17}$$

where the numerical coefficient Γ (which also enters into $^{EVW}\chi$) results from the details of the hyperfine interaction. The second term in the root can be quite large for small $\Delta\varepsilon$, and the quantity $^{EVW}\chi(\Delta\varepsilon,\delta)$ sets an upper limit for the seemingly diverging rate coefficients $^{FW}\bar{\chi}_s(\theta,\delta)$ at $\theta \to 0$. Note, however, that if the two K-components belong to different spin states of identical nuclei of the rotor, the first-order charge–dipole interaction vanishes, and both FW capture rate coefficients and their EVW counterparts become zero. Finally, we mention that the intermediate non-adiabatic regime between the sudden and the adiabatic limits in a situation similar to K-doubling was elaborated in Auzinsh et al. [22] for the case of the Λ-doubling in the application to the capture of $NO(X^2\Pi_{1/2}, j)$ by an ion.

4. Classical AC probabilities, cross-sections and rate coefficients

Within the AC approximation, the anisotropic effective potential in Equation (4) is replaced by its expectation value for given quantum numbers J, j, m; see Equation (5). In

this way, we get

$$^{\mathrm{AC}}\upsilon_m^{(J,j)}(\rho) = \frac{^{\mathrm{AC}}c_m^{(J,j)}(\delta)}{2\rho^2} - \frac{1}{2\rho^4}, \tag{18}$$

with

$$^{\mathrm{AC}}c_m^{(J,j)}(\delta) = J(J+1) - 2m^2 + j(j+1) + 2\delta m/\sqrt{j(j+1)}. \tag{19}$$

For a classical approximation of the relative motion, the capture probabilities are approximated by step-functions Θ when the collision energy $\kappa^2/2$ exceeds the height of the effective potential in Equation (18), i.e.

$$^{\mathrm{AC}}P_m^{(J,j.)}(\kappa,\delta) = \Theta\left(2k - {}^{\mathrm{AC}}c_m^{(J,j)}(\delta)\right). \tag{20}$$

Within yet another approximation, which is used in many applications [13–15], J is assumed to be large, and the terms $2m^2$ and $j(j+1)$ are neglected in comparison with $J(J+1) \approx J^2$. In this approximation, which will be called the classical AC (ACCl) approach, the expression for the transition probability assumes the form

$$^{\mathrm{ACCl}}P_m^{(J,j.)}(\kappa,\delta) = \Theta(2k - 2\delta m/\sqrt{j(j+1)} - J^2). \tag{21}$$

Equation (21) yields the maximum J for capture, $\tilde{J}_m$, as

$$\tilde{J}_m^2(\kappa,\delta) = (2\kappa - 2\delta m/\sqrt{j(j+1)})\Theta \times (1 - \delta m/\kappa\sqrt{j(j+1)}), \tag{22}$$

where the step-function Θ opens (or closes) m-specific capture channels.

Writing

$$^{\mathrm{ACCl}}\chi_j(\kappa,\delta) = \frac{1}{2\kappa(2j+1)}\sum_{m=-j}^{j}\int_0^{\infty} {}^{\mathrm{ACCl}}P_m^{(J,j.)}(\kappa,\delta)2JdJ \tag{23}$$

and performing the integration over J, we get

$$^{\mathrm{ACCl}}\chi_j(\kappa,\delta) = \frac{1}{(2j+1)}\sum_{m=-j}^{j}\left(1 + \frac{\delta m}{\kappa\sqrt{j(j+1}}\right)\Theta \times \left(1 + \frac{\delta m}{\kappa\sqrt{j(j+1}}\right). \tag{24}$$

The consecutive opening of capture channels produces slight undulations in the dependence of $^{Cl}\chi_j(\kappa,\delta)$ on κ. The undulations disappear in the large j-limit of Equation (21), which is given by

$$^{\mathrm{ACCl}}\chi_{j\gg1}(\kappa,\delta) = 1 + \left(-\frac{1}{2} + \frac{\kappa}{4\delta} + \frac{\delta}{4\kappa}\right)\Theta(\delta - \kappa). \tag{25}$$

To be consistent with the j-independence of the FW rate coefficients of Section 4, in what follows, Equation (25) is used for any j. Note that, for $\kappa < \delta$, only half of the Langevin contribution survives since the other half is quenched by the repulsive charge–dipole interaction.

The two limiting cases of Equation (25) are the Langevin limit

$$^{\mathrm{ACCl}}\chi(\kappa,\delta)_{j\gg1}\big|_{\delta=0} = 1 \tag{26}$$

and the charge–dipole dominated limit

$$^{\mathrm{ACCl}}\chi(\kappa,\delta)_{j\gg1}\big|_{\delta\gg\kappa} = {}^{\mathrm{ACCl,c\text{-}dip}}\chi(\kappa,\delta) == \frac{\delta}{4\kappa}. \tag{27}$$

The $1/\kappa$ divergence of $^{\mathrm{C\text{-}dip}}\chi(\kappa,\delta)$ at small κ can be traced back to the fact that the finite target area (i.e. the non-zero range of impact parameters) corresponds to capture without potential barrier. We note in passing that δ in the numerator on the r.h.s. of Equation (27) equals twice the number of the ACCl channels, $2^{\mathrm{ACCl}}N$, open for capture in the limit $\kappa \to 0$. This can be directly seen by calculating $^{\mathrm{ACCl}}N$ in the high-j limit as

$$^{\mathrm{ACCl}}N = \frac{1}{2j}\int_{-j}^{j}\tilde{J}_m^2(\kappa,\delta)\big|_{\kappa=0}dm = \delta/2. \tag{28}$$

Within the classical collision picture, Equation (25) is meaningful only for $\delta \gg 1$. Nonetheless, it is noteworthy that, for small κ, the asymptotics of $^{\mathrm{ACCl}}\chi(\kappa,\delta)$ with $\delta = 2$, i.e., $^{\mathrm{ACCl}}N = 1$ coincides with the s-wave unitary limit where the capture probability in a single open capture channel equals unity.

The thermal counterpart of Equation (25) is

$$^{\mathrm{ACCl}}\bar{\chi}_j(\theta,\delta) = \int_0^{\infty} {}^{\mathrm{ACCl}}\chi_j(\kappa,\delta)F(\kappa,\theta)d\kappa. \tag{29}$$

Explicit calculation yield [23]

$$^{\mathrm{ACCl}}\bar{\chi}_{j\gg1}(\theta,\delta) = = 1 + \frac{1}{2\sqrt{\pi}}\frac{\delta}{\sqrt{2\theta}} + \frac{1}{2\sqrt{\pi}}\frac{\sqrt{2\theta}}{\delta}\left(1 - \exp(-\delta^2/2\theta)\right) - \frac{1}{2}\mathrm{Erf}\left(\frac{\delta}{\sqrt{2\theta}}\right), \tag{30}$$

where $\mathrm{Erf}(x)$ is the error function. The limiting expressions for ${}^{\mathrm{ACCl}}\bar{\chi}(\theta,\delta)$ are

$$ {}^{\mathrm{ACCl}}\bar{\chi}(\theta,\delta) = \begin{cases} 1, & \text{for } \delta/\sqrt{\theta} \ll 1 \\ \delta/2\sqrt{2\pi\theta} & \text{for } \delta/\sqrt{\theta} \gg 1 \end{cases} . \quad (31) $$

Graphs of ${}^{\mathrm{ACCl}}\bar{\chi}(\theta,\delta)$ for $\delta \geq 4$ in the region of interplay between the asymptotics given by Equation (31) are shown in Figure 1 by full green lines. The graph of ${}^{\mathrm{ACCl}}\bar{\chi}(\theta,\delta)\big|_{\delta=2}$, extended to small θ until the convergence to its asymptotics in Equation (31), corresponds to the dashed green line.

5. Relation between FW and ACCl capture rate coefficients

The FW approach performs well under the condition $\kappa \ll 1$ and $\delta \leq 1$, while the ACCl approximation requires $\kappa \gg 1$ and $\delta \gg 1$. Though these conditions are mutually exclusive, one expects that the *s*-wave (i.e. FW) and classical (i.e. ACCl) rate coefficients will show some kind of relation, as was found earlier for capture in the field of isotropic charge-induced dipole interaction [24]. We consider now the simplest case when FW capture occurs in the first channel being completely open but still below the second threshold (i.e. the FW rate constant is maximal) and ACCl capture corresponds on average to one open channel (i.e. the minimum meaningful ACCl rate coefficient), ${}^{\mathrm{ACCl}}N = 1$. The respective rate coefficients are ${}^{\mathrm{FW}}\bar{\chi}_s^{\max}(\theta)$ (see Equation (16)) and ${}^{\mathrm{ACCl}}\bar{\chi}^{\min}(\theta) \equiv {}^{\mathrm{ACCl}}\bar{\chi}(\theta,\delta)\big|_{\delta=2}$ (see Equations (25) and (30)), in Figure 1 represented by the blue and the green dashed line, respectively. The range between the two lines will presumably be filled by the contributions from higher capture waves. We can thus anticipate that the classical expression given by Equations (25) and (30), for $\delta = 2$, will provide a reasonable approximation to the all-wave quantum capture rate coefficient for quite low temperatures.

An example that illustrates the transition between the FW and the ACCl regime under conditions close to that discussed above is provided by the capture of a proton by CH_3Din the rotational state $j = 2, k = 1$ that occurs in the lowest capture channel $J = 2$. We consider two different values of the dipole moment of CH_3D, $\mu_D = 1.6 \cdot 10^{-3}$ D [21] and $\mu_D = 2.19 \cdot 10^{-3}$ D [25]. These two values of μ_D correspond to two values of δ, $\delta_c = 1.11$ and $\delta_c = 1.52$, respectively. Both values of δ_c are above the upper limit of δ studied in Section 2, but presumably they are below the threshold values of $\delta_{\mathrm{th}}^{(J,j)}$ that correspond to the opening of the next capture channels, with $J = 1$, 2 and 3. A rough estimate of $\delta_{\mathrm{th}}^{(J,i)}$ within the AC approximation can be made by the condition

$$ {}^{\mathrm{AC}}c_m^{(J,j)}\left({}^{\mathrm{AC}}\delta_{\mathrm{th}}^{(J,j)}\right) = -1/4. \quad (32) $$

In this equation, $j = 2$ and $J = 1$, 2 and 3, while m is chosen from the condition that ${}^{\mathrm{AC}}\delta_{\mathrm{th}}^{(J,j)}$ found from this equation is minimal with respect to m. Of course, the triad $J = j = 2, m = -2$ is excluded from possible sets of J, j, m since it corresponds to the threshold for opening of the first capture channel where the AC approximation certainly is not applicable. In this way, one finds ${}^{\mathrm{AC}}\delta_{\mathrm{th}}^{(1,2)} = 7.66$, ${}^{\mathrm{AC}}\delta_{\mathrm{th}}^{(2,2)} = 12.5$ and ${}^{\mathrm{AC}}\delta_{\mathrm{th}}^{(3,2)} = 6.28$. Since these threshold values are noticeably higher than the values of δ_c given above, we expect that the rate coefficients for the capture $CH_3D(j = 2, k = 1) + H^+$ in the FW channel $J = j = 2$, $m = -2$ is given by its unitary limit, ${}^{\mathrm{FW}}\bar{\chi}_s^{\max}(\theta)$, for both values of δ_c, i.e., for those θ where the partial *s*-wave contribution to the total rate coefficient exceeds the contribution from higher waves (i.e. at ultra-low temperatures). Taking the upper limit of θ as 0.1, we find from Equation (24) that with $\alpha(CH_4) = 17.3$a.u. and $\mu(CH_3D + H^+) = 1.7 \cdot 10^3$a.u., this value of θ corresponds to $T = 6.2 \cdot 10^{-4}$K.

For smaller δ, a relation between the FW and the ACCl limit becomes uncertain since the AC approximation, for $\delta < 1$, cannot reproduce the effects (though small) of the charge–dipole interaction in the capture rate coefficient. If these effects are disregarded (i.e. if the limit $\delta \to 0$ is considered), a simple relation between the *s*-wave and classical capture rates can be given; see Dashevskaya et al. [24].

6. Conclusion

In its application to the dynamics of collisions between ions and dipolar symmetric top molecules, the present work has considered capture for the *s*-wave quantum and classical limits under the condition that the adiabatic approximation with respect to rotational transitions is applicable. In terms of temperature, these two limits correspond to the ultra-low and moderate temperature ranges defined in Nikitin and Troe [9]. The results obtained contribute to a better understanding of collisional aspects of the cold molecule physics and chemistry [27].

We have studied the properties of rate coefficients across a wide range of temperatures characterised by the dimensionless parameter θ, which is related to the conventional temperature T by Equation (15). Judging from our earlier work [20], we tentatively take the value $\theta = \theta_{\mathrm{th}} = 0.1$ as a 'threshold' for the characterisation of the transition between the classical ($\theta > \theta_{\mathrm{th}}$) and the quantum ($\theta < \theta_{\mathrm{th}}$)collision regime. Besides θ, the nature of the quantum effects depends on the value of parameter δ from Equation (3). If δ is not too small, the capture rate is controlled by the contribution from several partial waves, with the maximum value of the quantum number of total angular momentum $J = J_c \approx \sqrt{\delta}$. Here, the quantum effects are mainly related to the abrupt opening of the capture channels for pure charge–dipole interaction; these effects can be described by

a modification of the AC approach. If, on the other hand, δ is small ($\delta < 1$), the capture is determined by the lowest capture channel only. Here, the quantum effects are due to the interplay of charge–dipole and Coriolis interactions; these effects can be accounted for by the FW approximation. For the $CH_3D(j, k) + H^+$ system discussed in Section 5 and for different j, k states of CH_3D, the value of δ falls into the intermediate range.

Passing from our reference $CH_3D + H^+$ system to other cases, one, for example, can replace the proton by a heavier ion or replace the H atoms in the molecule by heavier atoms. In the former case, the replacement (say $H^+ \rightarrow F^+$) will decrease the quantum threshold T_{th} and increase δ, thus moving the system more towards classical conditions and minimising possible quantum effects. In the latter case, the replacement (say H → F) leaves the quantum threshold T_{th} unchanged, but strongly decreases δ because of a weak effect of isotopic substitution that produces a non-vanishing dipole moment. This case certainly falls into the FW regime discussed in this work. However, the question remains whether even at temperatures as low as μK can one still discern the small charge–dipole increment to the capture rate coefficient on a background of its Vogt–Wannier limit. We finally note that our approach does not allow to exactly trace the passage from the FW (ultra-low temperatures) to the ACCl (moderate temperature) regime, since this would require the consideration of contributions of several partial waves (not only one as in the FW case or many as in the AC case) and full interplay between the electrostatic and the Coriolis interactions. The numerical calculation of capture rate coefficients that bridges the gap between the FW and the AC limit and which is based on a full axially nonadiabatic channnel numerical treatment (with higher-wave contributions taken into account) is presented elsewhere [28].

Acknowledgements

This work acknowledges many stimulating discussions with Professor Martin Quack and his continuing interest in our work. Financial support from the European Office of Aerospace Research & Development (EOARD) (grant award FA 8655-11-3077) as well as discussions and technical help by I. Litvin are acknowledged as well.

References

[1] M. Quack and J. Troe, in *Encyclopedia of Computational Chemistry*, edited by P.V. Schleyer, N.L. Allinger, T. Clark, J. Gasteiger, and P.A. Kollmann (Wiley, Chichester, UK, 1978). Vol. **4**, p. 2708.
[2] H. Hotop, M.-W. Ruf, M. Allan, and I.I. Fabrikant, Adv. At. Mol. Opt. Phys. **49**, 85 (2003).
[3] M. Quack and J. Troe, Ber. Bunsenges. Phys. Chem. **78**, 240 (1974); **79**, 469 (1975).
[4] K. Sakimoto and K. Takayanagi, J. Phys. Soc. Jpn **48**, 2076 (1980).
[5] D.R. Bates, Proc. Roy. Soc. London A **384**, 289 (1982).
[6] D.C. Clary, Mol. Phys. **54**, 605 (1985).
[7] J. Troe, in *State-Selected and State-to-State Ion-Molecule Reaction Dynamics*, *Part 2: Theory*, edited by M. Baer and C.Y. Ng (Wiley, New York, 1992); Adv. Chem. Phys. **82**, 485 (1992).
[8] M. Ramillon and R. McCarroll, J. Chem. Phys. **101**, 8697 (1994).
[9] E.E. Nikitin and J. Troe, Phys. Chem. Chem. Phys. **7**, 1 (2005).
[10] A. Berengolts, E.I. Dashevskaya, E.E. Nikitin, and J. Troe, Chem. Phys. **195**, 271, 283 (1995).
[11] E.I. Dashevskaya, I. Litvin, E.E. Nikitin and J. Troe, Mol. Phys. **108**, 873 (2010).
[12] E.E. Nikitin and J. Troe, J. Phys. Chem. A **114**, 9762 (2010)
[13] J. Troe, J. Chem. Phys. **87**, 2773 (1987).
[14] S.C. Smith and J. Troe, J. Chem. Phys. **97**, 5451 (1992).
[15] J. Troe, J. Chem. Phys. **105**, 6249 (1996)
[16] M. Auzinsh, E.I. Dashevskaya, I. Litvin, E.E. Nikitin, and J. Troe, J. Phys. Chem. A **115**, 5027 (2011)
[17] R.N. Zare, *Angular Momentum* (Wiley, New York, 1988).
[18] L.D. Landau and E.M. Lifshitz, *Quantum Mechanics* (Pergamon Press, Oxford, 1977).
[19] E.I. Dashevskaya, I. Litvin, E.E. Nikitin, and J. Troe, Phys. Chem. Chem. Phys. **10**, 1270 (2008).
[20] E.I. Dashevskaya, I. Litvin, E.E. Nikitin, and J. Troe, J. Phys. Chem. A **115**, 6825 (2011).
[21] S.C. Wofsy, J.S. Muenter, and W. Klemperer, J. Chem. Phys. **53**, 249 (1970).
[22] M. Auzinsh, E.I. Dashevskaya, I. Litvin, E.E. Nikitin and J. Troe, J. Chem. Phys. **130**, 014304. (2009)
[23] E.I. Dashevskaya, I. Litvin, E.E. Nikitin and J. Troe, J. Phys. Chem. A **113**, 14212 (2009).
[24] E.I. Dashevskaya, A.I. Maergoiz, J. Troe, I. Litvin, and E.E. Nikitin, J. Chem. Phys. **118**, 7313 (2003).
[25] Y.H. Hollenstein, R.R. Marquardt, M. Quack, and M.A. Suhm, J. Chem. Phys. **101**, 3588 (1994).
[26] A.A. Radzig and B.M. Smirnov, *Reference Data on Atoms, Molecules, and Ions*, Springer Series in Chemical Physics, **31** vols. (Springer, Berlin, 1985).
[27] R.V. Krems, W.C. Stwalley, and B. Friedrich, editors, *Cold Molecules* (CRC Press, Boca Raton, FL, 2009).
[28] E.I. Dashevskaya, I. Litvin, E.E. Nikitin and J. Troe, submitted to publication.

Appendix. Symmetric top rotors with small dipole moments

A spherical top AB_n in its ground vibrational state has a vanishing dipole moment due to the mutual compensation of the dipole moments of the AB bonds. With isotopic substitution, B→B', the spherical top AB_n becomes a symmetric top with a non-zero dipole moment. The main contribution to the dipole moment increment comes from the change in the zero-point average of the AB distance upon substitution B→B':

$$\Delta\mu_D(\mathrm{AB/AB'}) \approx \left.\frac{\partial\mu_D(\mathrm{AB})}{\partial r_{\mathrm{AB}}}\right|_{r_{\mathrm{AB}}=r_{\mathrm{AB,e}}} \times \langle\Delta r\rangle_{00}\,. \qquad \langle\Delta r\rangle_{00} = \langle r_{\mathrm{AB}}\rangle_{00} - \langle r_{\mathrm{AB'}}\rangle_{00} \tag{A.1}$$

For a rough estimation, we consider Morse potentials for the individual AB bonds as

$$U(r_{\mathrm{AB}}) = D[1 - \exp(-\beta(r_{\mathrm{AB}} - r_{\mathrm{AB,e}})]^2 - D. \tag{A.2}$$

Writing $\langle r_{\mathrm{AB}}\rangle_{00} = r_{\mathrm{AB,e}} + \langle \Delta r_{\mathrm{AB}}\rangle_{00}$ and $\langle r_{\mathrm{AB'}}\rangle_{00} = r_{\mathrm{AB',e}} + \langle \Delta r_{\mathrm{AB'}}\rangle_{00}$, we obtain

$$\langle \Delta r_{\mathrm{AB}}\rangle_{00} = \frac{5}{8}\frac{\hbar\omega_{\mathrm{AB,e}}}{D\beta}, \tag{A.3}$$

with $\hbar\omega_{\mathrm{AB,e}}$ being the small-amplitude vibrational frequency of the isolated AB bond.

Substituting $\langle \Delta r_{\mathrm{AB}}\rangle_{00}$ and $\langle \Delta r_{\mathrm{AB'}}\rangle_{00}$ into Equation (4), and roughly approximating $(\partial\mu_D/\partial r_{\mathrm{AB}})_{r_{\mathrm{AB}}=r_{\mathrm{AB,e}}}$ by $\mu_D/r_{\mathrm{AB,e}}$, we get

$$\frac{\Delta\mu_D}{\mu_D} \approx \frac{5}{4}\frac{\hbar\omega_{\mathrm{AB,e}}}{2D\beta r_{\mathrm{AB,e}}}\left(1-\sqrt{M_{\mathrm{AB}}/M'_{\mathrm{AB'}}}\right), \tag{A.4}$$

where M_{AB} and $M_{\mathrm{AB'}}$ are the reduced masses of the bonds AB and AB'. Introducing the anharmonicity constant $x_{\mathrm{AB,e}} = \hbar\omega_{\mathrm{AB,e}}/4D$ and the zero-point harmonic vibrational amplitude $\Delta r_{\mathrm{AB0}} = \sqrt{\hbar/M_{\mathrm{AB}}\omega_{\mathrm{ABe}}}$, we rewrite Equation (A.1) in the form

$$\frac{\Delta\mu_D}{\mu_D} = \frac{\Delta r_{\mathrm{AB0}}}{r_{\mathrm{AB,e}}}\frac{5}{4}\sqrt{2x_{\mathrm{AB,e}}}\left(1-\sqrt{M_{AB}/M'_{AB'}}\right), \tag{A.5}$$

which indicates the reason for the small magnitude of the ratio $\Delta\mu_D/\mu_D$, being the small zero-point harmonic vibrational amplitude in comparison with the equilibrium distance of the AB bond and the small value of the anharmonicity constant for the AB oscillator. The last factor on the right-hand side of Equation (A.4) also can be small, provided that the ratio $M_{\mathrm{AB}}/M'_{\mathrm{AB'}}$ is close to unity, since $1-\sqrt{M_{\mathrm{AB}}/M_{\mathrm{AB'}}} \propto \Delta M_{\mathrm{AB/AB'}}/M_{\mathrm{AB}}$, with $\Delta M_{\mathrm{AB/AB'}}$ being the change in the reduced mass of the AB fragment upon isotopic substitution.

Considering CH_3D as an example, we employ parameters of CH from Radzig and Smirnov [26] for the characterisation of the individual CH bonds. This yields an estimate of the increment, upon substitution H→D, of the dipole of CD as $\Delta\mu_D(\mathrm{CH/CD}) \approx 8\cdot 10^{-3}$D, which can be compared with $\mu_D(\mathrm{CH_3D}) = 5.6\cdot 10^{-3}$D from high-resolution interferometric Fourier transform experiments [25] and $\mu_D(\mathrm{CH_3D}) = 6.8\cdot 10^{-3}$D from quantum Monte Carlo calculations [25].

For capture of CH_3D by H^+, δ is bracketed between 1 and 2 (see Section 5). This is an intermediate value, since δ can be much larger if the proton is replaced by a heavier ion, or much lower if the CH/CD moiety is replaced by a AB/AB′ moiety with smaller change in the reduced mass upon isotopic substitution. Thus, the interesting range of δ corresponds to wide variations in δ, from values much lower to much higher than unity.